Article

Not peer-reviewed version

Kisspeptin Alleviates Human Hepatic Fibrogenesis by Inhibiting TGFb Signaling in Hepatic Stellate Cells

Kavita Prasad [†] , Dipankar Bhattacharya [†] , Shams Gamal Eldin Shams [†] , Kimberly Izarraras , Tia Hart , Brent Mayfield , Maryjka B. Blaszczyk , Zhongren Zhou , Utpal B. Pajvani , Scott L. Friedman , Moshmi Bhattacharya [*]

Posted Date: 14 September 2024

doi: 10.20944/preprints202409.1111.v1

Keywords: KISS1R; kisspeptin; MASLD; MASH; fibrosis, hepatic stellate cells; TGFβ

Article

Kisspeptin Alleviates Human Hepatic Fibrogenesis by Inhibiting TGFβ Signaling in Hepatic Stellate Cells

Kavita Prasad [1,†], Dipankar Bhattacharya [2,†], Shams Gamal Eldin Shams [3,†], Kimberly Izarraras [4], Tia Hart [5], Brent Mayfield [6], Maryjka B. Blaszczyk [7], Zhongren Zhou [8], Utpal B. Pajvani [9], Scott L. Friedman [10] and Moshmi Bhattacharya [11,*]

[1] Department of Medicine, Robert Wood Johnson Medical School, Rutgers University, New Brunswick, NJ, USA; kp460@connect.rutgers.edu
[2] Division of Liver Diseases, Icahn School of Medicine at Mount Sinai, New York, NY, USA; dipankar.bhattacharya@mssm.edu
[3] Department of Medicine, Robert Wood Johnson Medical School, Rutgers University, New Brunswick, NJ, USA; ss4459@rwjms.rutgers.edu
[4] Department of Medicine, Robert Wood Johnson Medical School, Rutgers University, New Brunswick, NJ, USA; ki113@gsbs.rutgers.edu
[5] Department of Medicine, Robert Wood Johnson Medical School, Rutgers University, New Brunswick, NJ, USA; tmh187@cinj.rutgers.edu
[6] Department of Medicine, Columbia University, New York, NY, USA; bcm2151@cumc.columbia.edu
[7] Department of Pathology and Laboratory Medicine, Robert Wood Johnson Medical School, Rutgers University; mb2001@rwjms.rutgers.edu
[8] Department of Pathology and Laboratory Medicine, Robert Wood Johnson Medical School, Rutgers University; zz442@rwjms.rutgers.edu
[9] Department of Medicine, Columbia University, New York, NY, USA; up2104@cumc.columbia.edu
[10] Division of Liver Diseases, Icahn School of Medicine at Mount Sinai, New York, NY, USA; scott.friedman@mssm.edu
[11] Department of Medicine, Robert Wood Johnson Medical School, Rutgers University, New Brunswick, NJ, USA;mb1722@rutgers.edu
* Correspondence: mb1722@rutgers.edu
† authors contributed equally.

Abstract: The peptide hormone kisspeptin attenuates liver steatosis, metabolic dysfunction-associated steatohepatitis (MASH) and fibrosis in mouse models, by signaling via the kisspeptin 1 receptor (KISS1R). However, whether kisspeptin impacts fibrogenesis in the human liver is not known. We investigated the impact of a potent kisspeptin analog (KPA) on fibrogenesis using human precision cut liver slices (hPCLS) from fibrotic livers from male patients, in human hepatic stellate cells (HSCs), LX-2 and in primary mouse HSCs. In hPCLS, 48 h and 72 h of KPA (3 nM, 100 nM) treatment decreased collagen secretion, and lowered expression of fibrogenic and inflammatory markers. Immunohistochemical studies revealed that KISS1R is expressed and localized to HSCs in MASH/fibrotic livers. In HSCs, KPA treatment reduced transforming growth factor β (TGFβ)–induced expression of fibrogenic and inflammatory markers, in addition to decreasing TGFβ–induced collagen secretion, cell migration, proliferation and colony formation. Mechanistically, KISS1R signaling downregulated TGFβ signaling by decreasing SMAD2/3 phosphorylation, via activation of protein-phosphatases PP2A, that dehosphorylates SMAD 2/3. This study revealed for the first time that kisspeptin reverses human hepatic fibrogenesis thus identifying it as a new therapeutic target to treat hepatic fibrosis.

Keywords: KISS1R; kisspeptin; MASLD; MASH; fibrosis; hepatic stellate cells; TGFβ

 doi:10.20944/preprints202409.1111.v1

1. Introduction

Metabolic dysfunction-associated steatotic (fatty) liver disease (MASLD), previously known as non-alcoholic fatty liver disease (NAFLD), is an escalating health problem with a global prevalence of 25%[1]. The leading risk factors of MASLD are obesity, insulin resistance, type 2 diabetes, and other metabolic abnormalities collectively termed metabolic syndrome. A hallmark feature of MASLD is excessive fat accumulation or steatosis in hepatocytes, due to dysregulated fat metabolism. MASLD can progress to metabolic dysfunction-associated steatohepatitis (MASH), previously known as nonalcoholic steatohepatitis (NASH), which is characterized by hepatocyte inflammation and injury. As the disease progresses, patients can develop fibrosis, cirrhosis and liver cancer. Liver fibrosis, which predicts mortality and disease severity[2], is characterized by excessive deposition of extracellular matrix proteins such as type 1 collagen, leading to distorted hepatic architecture. Fibrosis results from the activation of hepatic stellate cells (HSCs), which are the major fibrogenic cell type in the liver. Activated HSCs acquire the characteristics of mesenchymal fibroblast cells and produce various extracellular matrix constituents, such as collagen, fibronectin, and α-smooth muscle actin (α-SMA). The liver eventually ceases to function due to excessive scar production. Some patients can progress to hepatocellular carcinoma (HCC)[3], a fatal cancer that is on the rise[4]. In females, MASH is now the leading cause of liver transplant, and second to alcoholic liver disease, in males[5]. Thus, there is a direct need for the development of new therapeutics to treat MASH with fibrosis.

Kisspeptins are peptide hormones, encoded by the KISS1 gene, that circulate in the blood and bind to and signal via the Gαq/11 protein-coupled receptor, kisspeptin 1 receptor (KISS1R)[6; 7]. The kisspeptin/KISS1R signaling system is expressed centrally in the brain and plays a key role in regulating puberty and reproduction, in addition to metabolism[6; 8; 9]. Peripherally, KISS1 and KISS1R are expressed in several metabolic tissues including the pancreas, adipose tissue, and liver[6; 10]. The liver produces kisspeptin, which has been shown to be a major regulator of insulin resistance in type 2 diabetes and gestational diabetes[11-15]. We have shown using a pre-clinical mouse model of MASH/fibrosis that kisspeptin administration reduced advanced (F3) hepatic fibrosis[11] in Diet Induced Animal Model of Non-Alcoholic Liver Disease (DIAMOND) mice[16], and decreased serum alanine aminotransferase (ALT) levels, a clinical biomarker for MASH that is indicative of liver injury[11]. Importantly, kisspeptin treatment of DIAMOND mice fed a high fat 'Western' diet (HFD) and sugar water exhibited a significant reduction in several inflammatory and profibrogenic markers [11], including transforming growth factor β1 (TGF β1), a critical mediator of hepatic fibrosis[17; 18] and decreased hepatic hydroxyproline levels (indicative of collagen content)[11]. However, whether activation of KISS1R directly regulates fibrogenesis is not known. In this work, we tested the hypothesis that kisspeptin directly attenuates pathways regulating HSC activation, to mediate its antifibrotic effects. We observed that KISS1R is expressed in HSCs in fibrotic livers from MASH patient biopsies. The effects of kisspeptin treatment were assessed in patients with fibrotic livers using the clinically relevant human precision cut liver slices (hPCLS) model. In this model, the morphological (e.g. cell types, architecture, heterogeneity) and biological (e.g extracellular matrix) organization of the native liver as well as the pathological features of the disease is preserved[19; 20]. We demonstrate that kisspeptin treatment of patient hPLCS and human and mouse HSCs decreased fibrogenic and inflammatory markers via KISS1R-mediated downregulated TGFβ–induced signaling in HSCs.

2. Materials and Methods

2.1. Human Precision-Cut Liver Slices

Human precision-cut liver slices (hPCLS) were generated as previously described[21] from surgically resected de-identified human fibrotic livers from three male patients (Table 1), following Institutional Review Board (IRB) approval at Icahn School of Medicine at Mount Sinai, New York City, N.Y. In each case, fibrotic regions adjacent to tumors were selected from patients with HCC, by a board-certified pathologist, to generate 8 mm diameter and 200 μm thick liver slices. Fresh medium was added daily containing either vehicle (PBS), TAK-448, a potent kisspeptin analog, henceforth

 doi:10.20944/preprints202409.1111.v1

referred to as KPA (3 nM, 100 nM), or 10 mM TGFβ receptor 1 kinase inhibitor II (Alk5i), (Calbiochem catalog #616452)[19], for the indicated times, after which the tissue was processed for measuring changes in protein expression using immunohistochemistry (see below). Additionally, total RNA was isolated from tissue using RNeasy Mini Kit (Qiagen, CA, USA) and used for measuring changes in gene expression by RT-quantitative PCR (qPCR), as described[21] (see below). Secreted collagen was assessed in culture media by human pro-collagen I alpha 1 ELISA (Abcam, ab210966), as described[21]. For cytotoxicity assessment, lactate dehydrogenase (LDH) and albumin levels were measured in the conditioned media, as previously described[21].

Table 1. Characteristics of human liver donors used for hPLCs studies.

Patient ID	Age (Years)	Sex	Diseases Background	Pathological diagnosis	Fibrosis Stage
1	76	Male	Patient has underlying HBV diagnosed with a mass in segment 5/6 of the liver (consistent with HCC)	Mild portal and mild interface hepatitis, compatible with the patient's history of hepatitis B	F1
2	66	Male	HCC (HBV infected chronic hepatitis)	Mild portal chronic inflammation and periportal fibrosis with bridging fibrous septa. No interface hepatitis or lobular inflammation and steatosis.	F2
3	53	Male	HCC (HCV infected chronic hepatitis)	Nodular liver parenchyma without significant portal or lobular inflammation, No significant steatosis.	F4

2.2. Human LX-2 Stellate Cell Culture and Treatment

The immortalized human hepatic stellate cell line, LX-2 were established in the laboratory of Dr. Scott Friedman at Icahn School of Medicine at Mount Sinai, NY, USA[22]. Cells were purchased from EMD Millipore (Burlington, MA) and cultured in Dulbecco's modified Eagle's medium supplemented with 10 % (v/v) fetal bovine serum (FBS). Prior to treatment, cells were serum-starved overnight to synchronize metabolic activity in serum-free DMEM (Thermo Fisher Scientific, Waltham, MA, USA). Cells were treated every 24 h with KPA (3 nM, 100 nM), purchased from MedChem Express (Monmouth Junction, NJ, USA); these concentrations were selected based on previous studies[11; 23]. KPA (3 nM) was added in the presence or absence of TGFβ (5ng/ml) (R&D Systems, Minneapolis MN).

2.3. Primary Mouse Hepatic Stellate Cell (HSCs) Culture and Treatment

Primary mouse hepatic stellate cells were isolated as previously described[24; 25] from C57Bl6/J mice and cultured in DMEM containing 10% FBS for 48 h in 12-well tissue culture plates (90, 000 cell/well). Medium was then replaced with serum-free medium containing KPA (3 nM) for an additional 48 h. Total RNA was extracted using TRIzol reagent (Thermo Fisher, Waltham, MA) and gene expression was determined using SYBR green RT-qPCR as described[11] (see below), using primers listed in Table S1.

2.4. Real Time PCR (RT-qPCR) Quantification of Gene Expression

Reverse transcription was done according to manufacturer's instructions using iScript RT Supermix (Bio-Rad). Gene expression was determined using SYBR green RT-qPCR as described previously[11] using primers listed in Table S1. For gene expression studies in LX-2 cells, cells were seeded in a 6-well plate (150,000 cells/well), serum starved overnight and then stimulated for 48 h. Total RNA was extracted using a RNeasy Mini Kit (Qiagen, CA, USA).

 doi:10.20944/preprints202409.1111.v1

2.5. RNA-Seq Data Analysis

LX-2 cells (150, 000/well) were plated in 6-well plates, serum starved overnight and then treated with either vehicle (PBS), KPA (3 nM) and/or TGFβ (5 ng/ml) for 48h. Total RNA was extracted using the RNeasy Mini Kit (Qiagen, CA, USA). The purity of RNA was assessed using 2100 Bioanalyzer instrument (Agilent, CA) at Albert Einstein College of Medicine Epigenomics Shared Facility. Purified RNA was used to prepare libraries using Qiaseq Stranded RNA lib Kit with UDI and QIAseq FastSelect -rRNA HMR Kit (Qiagen INC.) for Illumina sequencing. Libraries were QC using Fluorometric Quantitation (Qubit; Invitrogen:Thermo Fisher Scientific), Agilent 4150 TapeStation System and QPCR (Roche Light Cycler). RNASeq libraries were multiplexed and sequenced as 1 x 100 bp Single end on NEXTSEQ 2000 (Illumina) following standard protocols. The sequencing files in FASTQ format of each sample were trimmed for adaptors using trim galore v0.3.7, and then aligned against human genome hg38 using STAR aligner v2.7.9a. Aligned sequencing data were then converted to gene count matrices using STAR. Differential gene analyses were performed using R package DESeq2 v1.42.0, genes with more than 2-fold change and below 0.05 adjusted pvalue were considered significant differential. Gene set enrichment analysis was done using R package fgsea v1.28.0 against KEGG and GO database.

2.6. Immunoblot Analysis

Western blot analysis was conducted as previously described[11; 26; 27]. Briefly, cells were lysed in RIPA buffer containing protease inhibitors and total protein (50 μg) was extracted and separated using SDS-PAGE. Proteins transferred to nitrocellulose membranes were probed using the following anti-human antibodies: anti-rabbit KISS1 (Protein Tech catalog # 18375-1-AP; 1: 1000), anti-rabbit GPR54 (Abcam, catalog # ab137483; 1: 1000), anti-mouse fibronectin (R&D Systems, catalog # MAB19182; 1: 1000); the following antibodies were purchased from Cell Signaling Technologies (CST): anti-rabbit collagen (CST catalog # 91144-220; 1: 1000**),** anti-rabbit snail (CST catalog # 3895; 1: 1000), anti-rabbit Phospho SMAD2/3 (CST catalog # 8828) anti-rabbit SMAD2/3 (CST catalog # 8685) anti-mouse GAPDH (mAb catalog #97166), anti-rabbit SMA (CST catalog # 19245), anti-mouse b-actin (CST catalog # 3700T), anti-rabbit vinculin (CST catalog # 13901). Proteins on membranes were imaged using by chemiluminescence with Super Signal West Dura Extended Duration Substrate (catalog # 34076 Thermo Scientific, Waltham, MA) and ChemiDoc Touch imaging system (Bio-Rad, Hercules, CA) and subsequently quantified using Image Lab Software (Bio-Rad).

2.7. LX-2 Cell Proliferation Assay

LX-2 cells (5000 cells/well) were plated in a 96-well plate, serum-starved overnight and treated for 72h. Cell proliferation was determined using BrdU Cell Proliferation Kit (catalog #126556 Abcam, Cambridge, MA, USA), according to the manufacturer's instructions, as described[21]. Briefly, cells were incubated with BrdU reagent for 2 hours at 37 C, and proliferation quantified by measuring absorbance at 370 nm with reference wavelength at 492 nm.

2.8. LX-2 Cell Transformation Assay

Cell transformation assays were performed using soft-agar assay (3D) Cell Transformation Assay Kit (Colorimetric) (catalog #ab235698, Abcam, Cambridge, MA, USA) following the manufacturer's recommendations. Cells (4×10^4) were cultured in soft agar for 7 days at 37 C, after which absorbance was measured at 450 nm using a spectrophotometer, upon addition of the WST working solution.

2.9. Kisspeptin Secretion

Kisspeptin secretion assays were conducted as previously described[26]. Cells (5×10^5 cells/well) were grown in phenol red-free RPMI with 10% FBS for 24 h after which the conditioned media was collected and used for measuring secreted kisspeptin levels, using a fluorescent enzyme immunoassay (EIA) kit: Human KISS1 (68–121) Amide/Metastin (1–54) from Phoenix

 doi:10.20944/preprints202409.1111.v1

Pharmaceuticals Inc (CA) catalog #RK-04859, according to the manufacturer's instructions. Secretion was normalized to the protein concentration of cells in each well.

2.10. Immunohistochemistry of Human Liver

Immunohistochemistry was conducted on de-identified hPCLS, as described[21]. Briefly, sections (8 mm) were cut from fresh frozen tissue (OCT blocks), fixed in methacarn (60% methanol, 30% chloroform and 10% acetic acid) for 15 min at -20 C. After washing in TBS-T, sections were stained with primary antibody using anti-collagen 1 (1: 200, Rockland, catalog #600-401-103-0.1) and anti a-SMA (1: 200 Abcam Ab5694), overnight, followed by goat anti-rabbit Alexa Fluor 647 (1: 500; Invitrogen#A21245), for 1 hr. Sections were mounted using DAPI fluoromount-G (Southern Biotech, catalog#0100-20).

Immunohistochemistry was conducted on formalin fixed paraffin embedded (FFPE) human liver sections as described,[26; 27]. De-identified FFPE sections from pathologist verified MASH patients were obtained from archived liver tissue deposited at Robert Wood Johnson University Hospital Anatomic Pathology laboratory. Following deparaffinization and heat induced antigen retrieval, slides were incubated with primary antibodies: the rabbit anti-KISS1R (anti-GPR54: Abcam, ab137483; 1:250) and mouse anti-desmin (Abcam ab6322, 5 µg/ml) overnight. KISS1R immunoreactivity was detected using the Alexa Fluor 555 Tyramide SuperBoost Kit (ThermoFisher Scientific, catalog #B40923). Desmin immunoreactivity was detected using donkey anti-mouse Alexa Fluor 488 (1: 500; Invitrogen catalog #A-21202). A matched negative staining control, normal rabbit IgG polyclonal antibody (Sigma Aldrich, catalog #12-370, 1:100), was used to confirm the primary antibody specificity. All slides were processed in parallel. Images were acquired using a Zeiss LSM 700 laser scanning microscope.

2.11. Statistical Analysis

The differences between experimental and treated groups were determined using unpaired, two-tailed Student's t-test or one-way or two-way analys1is of variance (ANOVA), followed by post hoc Bonferroni's Multiple Comparison test (GraphPad Prism Software, Inc, La Jolla, CA). All values are expressed as mean ± SEM and a value of $P<0.05$ was considered statistically significant.

3. Results

3.1. Kisspeptin Analog, TAK-448 (KPA), Reduces Fibrogenic and Inflammatory Markers, as well as Collagen Secretion in Diseased Human Patient-Derived Precision Cut Liver Slices (hPCLS)

To test our hypothesis that kisspeptin has an anti-fibrotic effect in human liver, we utilized PCLS generated from the stromal (*fibrotic, non-tumor)* biopsies, from three male patients with HCC (Table 1). Liver slices were treated with the potent kisspeptin analog, TAK-448 (3 nM, 100 nM, henceforth referred to as KPA) for 48 h or 72 h. These KPA concentrations were selected since they decreased triglyceride accumulation and increased mitochondrial β-oxidation in primary mouse hepatocytes, and stimulated insulin secretion in isolated human pancreatic islets[11; 23]. Since the TGFβ receptor 1 kinase inhibitor II (Alk5i) exhibits anti-fibrogenic effects by targeting TGFβ signaling[19], we used ALK5i as a positive control in these studies. There was no impact of KPA or ALK5i on the viability of hPCLS (Figure S1). KPA treatment significantly lowered the mRNA levels of key fibrogenic genes *COL1A1* (encodes collagen), *ACTA2* (encodes a-smooth muscle actin, a-SMA) and *FN1* (encodes fibronectin), compared to control (PBS), in each patient (Figure 1A-I). A similar effect was observed with ALK5i. KPA treatment also significantly reduced collagen secretion by hPCLS (Figure 1 J-L), consistent with the effects on the level of *COL1A1* transcript (Figure 1 A-C).

To detect changes in fibrogenic protein expression following KPA treatment, immunohistochemical analysis was conducted. Results revealed that after 48 h and 72 h of KPA (3 nM, 100 nM) treatment, collagen 1 and a-SMA protein expression was reduced compared to untreated liver slices (Figure 2A-D, Figures. S2 and S3). These observations were similar to the effect of ALK5i treatment (Figure 2A-D, Figures S2 and S3). Evaluation of representative H&E-stained liver

 doi:10.20944/preprints202409.1111.v1

sections showed that 48 h of KPA treatment did not alter tissue architecture (Figure S4). Picrosirius red staining revealed the extent of fibrosis in each patient liver prior to any treatment as measured blindly by a pathologist, revealing F1, F2, and F4 stages of fibrosis for patients 1, 2, and 3, respectively (Figure S4, and Table 1).

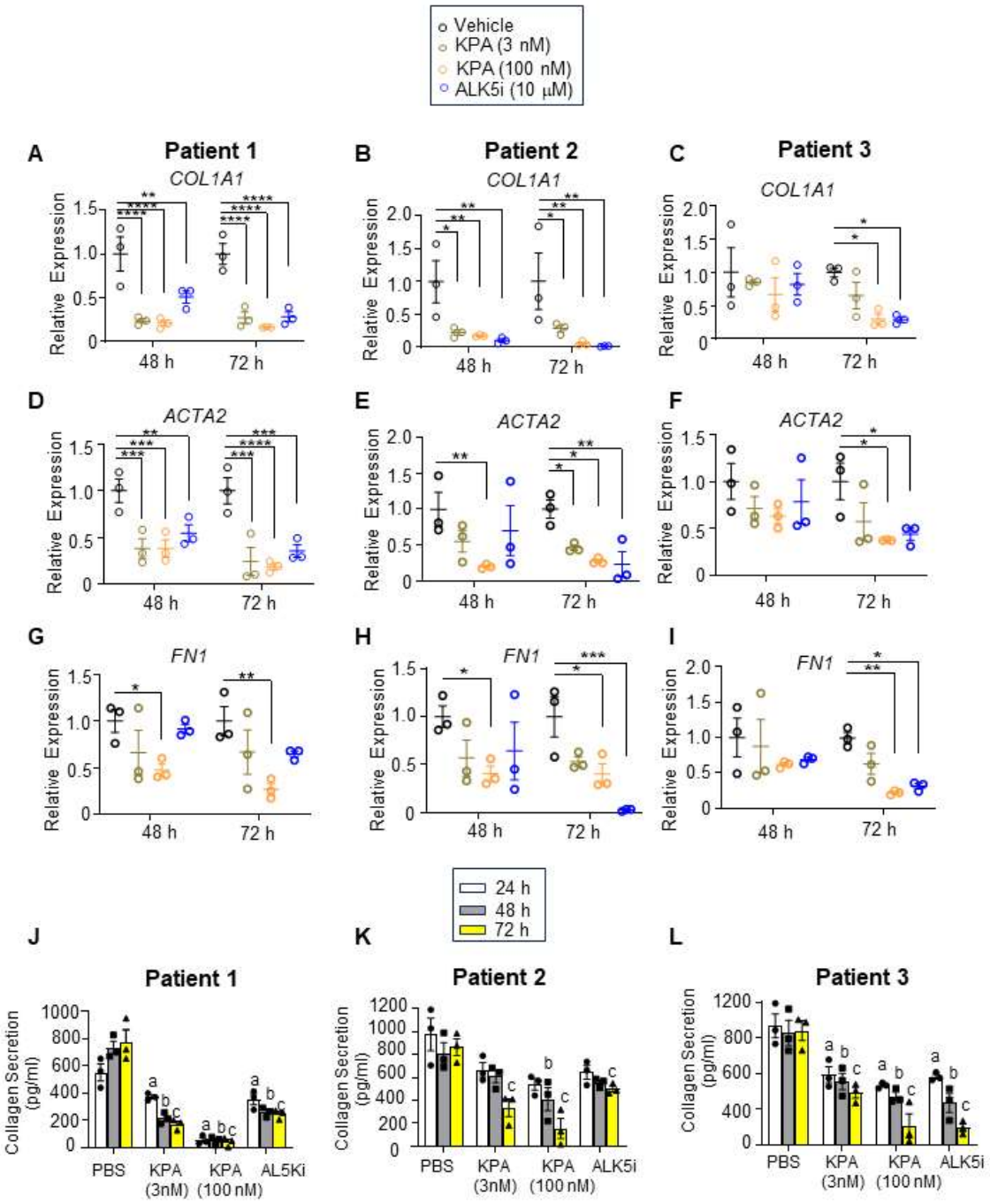

Figure 1. KPA reduces fibrogenic gene expression as well as type 1 collagen secretion in human fibrotic precision cut liver slices (PCLS). Human PCLS generated from patients with fibrotic livers were treated with KPA (3 nM, 100 nM), vehicle (PBS) or TGFβ receptor 1 kinase inhibitor II (Alk5i, 10 mM) for 48 or 72h. (A-I) Changes in fibrogenic gene expression determined by qPCR. (J-L) Secreted pro-collagen I alpha 1 protein in culture media measured by ELISA; a, $P < 0.05$ vs. PBS (vehicle) secretion (24 h); b, $P < 0.05$ vs. PBS (vehicle) secretion (48h); c, $P < 0.05$ vs. PBS (vehicle) secretion (72h). For A-I: results expressed as mean +/- S.E.M. *$p < 0.05$ vs control. **$p < 0.01$ vs control. ***$p < 0.001$ vs control. ****$p < 0.0001$ vs control. Two-way ANOVA followed by multiple comparison test.

Preprints.org (www.preprints.org) | NOT PEER-REVIEWED | Posted: 14 September 2024 doi:10.20944/preprints202409.1111.v1

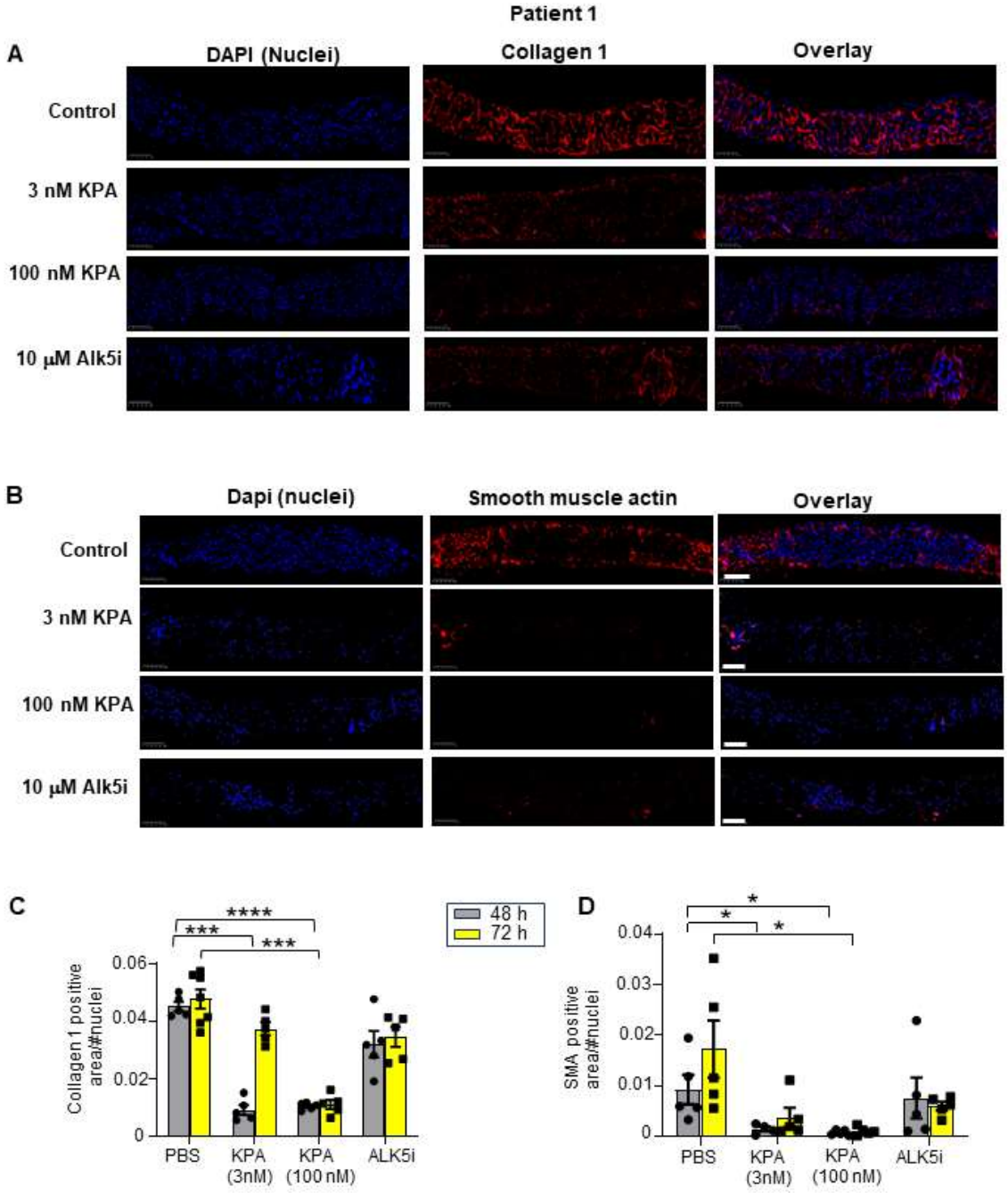

Figure 2. KPA treatment reduces collagen and smooth muscle actin (SMA) expression in hPCLS. Representative images of human PCLS generated from fibrotic liver biopsy from Patient 1, treated with KPA, vehicle (PBS) or ALK5i for 48h and immunostained for (A) collagen 1 and (B) smooth muscle actin. Scale bars: 250 mm. (C) Quantification of collagen and smooth muscle actin (SMA) immunostaining in hPLCS from Patient 1 treated with KPA (3 nM, 100 nM), vehicle (PBS) or ALK5i (10 mM) for 48h or 72h. See Figure S2 for additional images. Results: mean +/- S.E.M. *p < 0.05 vs control. **p < 0.01 vs control. ***p < 0.001 vs control. ****p < 0.0001 vs control. Two-way ANOVA followed by multiple comparison test.

Having observed that KPA reduced fibrogenesis, we assessed the effect of 48 h and 72 h KPA treatment on inflammatory markers. In both cases, KPA treatment robustly reduced the expression of interleukin-6 (*IL-6*) mRNA levels at 48 h, which was sustained at 72 h (Figure 3A-C), without any impact on drug toxicity (Figure S1). Similar effects were observed with ALK5i (Figure 3A-C; Figure

 doi:10.20944/preprints202409.1111.v1

S1). For tumor necrosis factor-a (*TNFA),* KPA only decreased *TNFA* mRNA levels at the higher dose in patients 1 and 2, with the effect being more pronounced after 72 h (Figure 3D-F). In patient 3, *TNFA* mRNA expression decreased in response to KPA (3 nM and 100 nM) and ALK5i treatment especially after 72 h, although statistical significance was not achieved. Taken together, these results reveal for the first time that KPA displays anti-fibrotic and anti-inflammatory properties in human fibrotic liver samples.

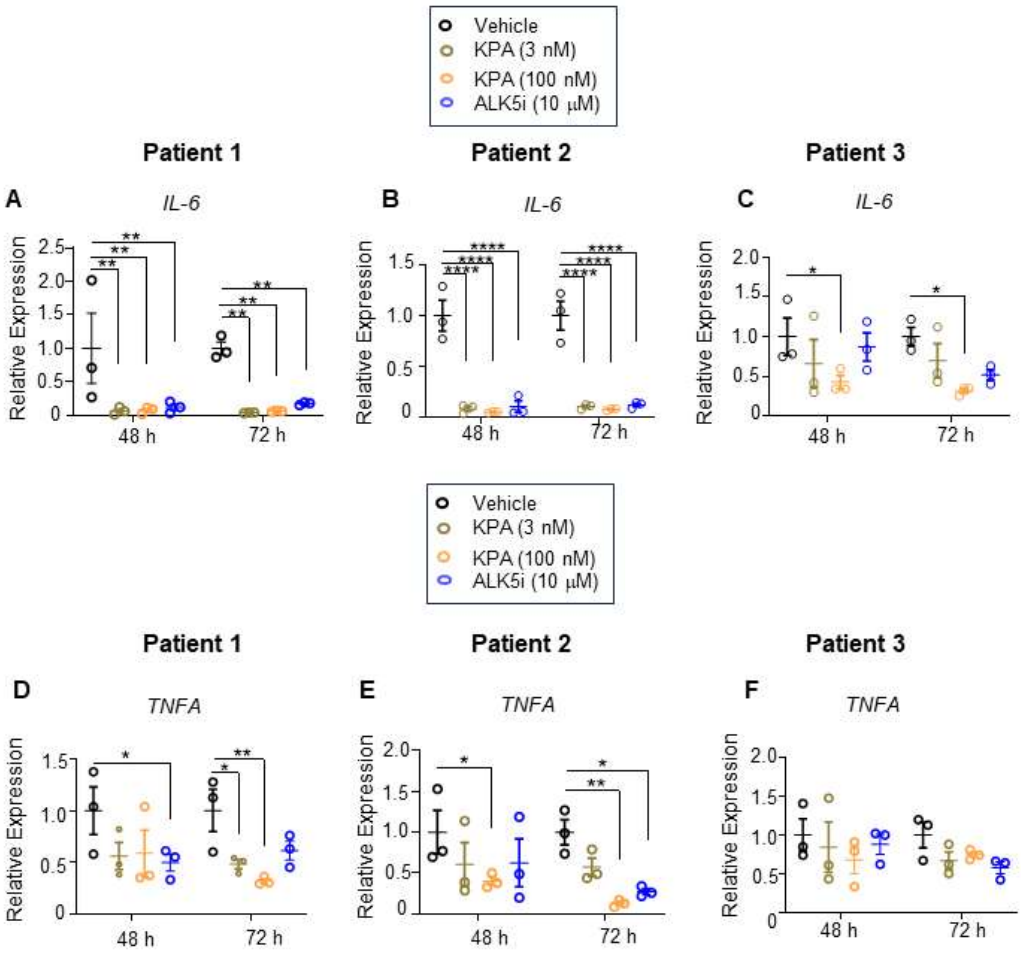

Figure 3. KPA reduces inflammatory gene expression in hPCLS. Human PCLS generated from patients with fibrotic livers were treated with KPA (3 nM, 100 nM), vehicle (PBS) or ALK5i (10 mM) for 48 or 72h. Changes in gene expression determined by qPCR for (A, D) Patient 1; (B, E) Patient 2 and (C, F) Patient 3. Results expressed as mean +/- S.E.M. *p < 0.05 vs control. **p < 0.01 vs control. ***p < 0.001 vs control. ****p < 0.0001 vs control. Two-way ANOVA followed by multiple comparison test.

3.2. KPA Treatment Upregulates KISS1 and KISS1R in hPCLS and KISS1R Is Strongly Expressed in Human HSCs

To further investigate the mechanistic actions of KPA in human liver slices, we examined the expression of *KISS1* and *KISS1R* mRNA levels and observed that 100 nM KPA significantly induced *KISS1* and *KISS1R* mRNA levels after 72 h of treatment (Figure 4A-F). In contrast, ALK5i treatment had no effect on *KISS1* and *KISS1R* transcript levels (Figure 4A-F). Additionally, using validated antibodies[11; 27; 28] immunohistochemical analysis of endogenous KISS1R in human livers from MASH patients with fibrosis revealed that KISS1R is robustly expressed in hepatic stellate cells (red) and colocalizes (yellow, overlay) with desmin (green), an intermediate filament marker of hepatic stellate cells[29] (Figure 4G). Taken together, these results lead us to conclude that activation of

 doi:10.20944/preprints202409.1111.v1

KISS1R has anti-fibrogenic roles and one potential mechanism by which KPA exerts a protective role is via the upregulation of *KISS1* and *KISS1R* levels in patient livers.

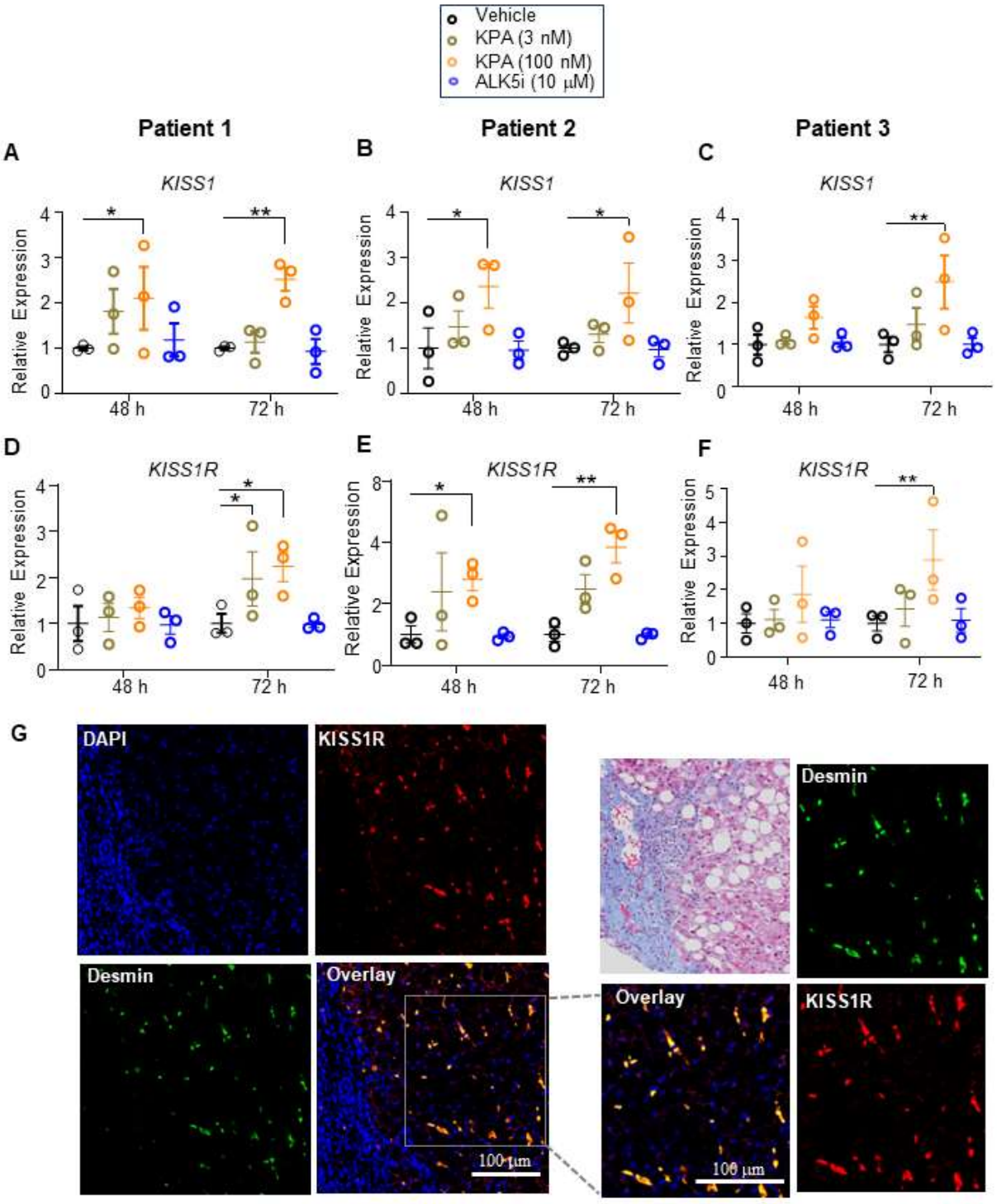

Figure 4. KPA treatment upregulates *KISS1* and *KISS1R* expression in hPCLS. Human PCLS generated from patients with fibrotic liver biopsies were treated with KPA (3 nM, 100 nM), vehicle (PBS) or ALK5i (10 mM) for 48 or 72h. Changes in **(A-C)** *KISS1* and *KISS1R* **(D-F)** gene expression as determined by qPCR in patient livers. Results expressed as mean +/- S.E.M. *p < 0.05 vs control. **p < 0.01 vs control. Two-way ANOVA followed by multiple comparison test. **(G)** Representative confocal images of human hepatic stellate cells in MASH patient biopsies, immunostained for endogenous KISS1R (red) and desmin (green), a marker for stellate cells. Areas of colocalization (yellow) shown in overlay; magnified images and trichtome staining of liver fibrotic section shown on the right.

 doi:10.20944/preprints202409.1111.v1

3.3. KPA Treatment Attenuates Fibrogenesis in Hepatic Stellate Cells (HSCs)

To better understand the anti-fibrotic roles of KISS1R signaling in the liver, we used the immortalized human hepatic stellate cell line, (LX-2), a highly established cellular model of human hepatic fibrogenesis[22]. To initiate these studies, we first quantified KISS1 and KISS1R protein levels in the LX-2 cells. We used the human MDA-MB-231 and SKBR3 breast cancer cell lines as positive controls for analyzing KISS1 and KISS1R protein levels. We have previously shown that MDA-MB-231 cells express high endogenous levels of KISS1 and KISS1R[26-28]. In contrast, native (parental) SKBR3 cells do not, but when KISS1R is stably expressed in these cells (KISS1R-SKBR3), it leads to robust expression of KISS1R, as well as KISS1, and kisspeptin secretion[26; 28]. We observed that LX-2 cells express KISS1 and KISS1R protein endogenously at levels similar to MDA-MB-231 and KISS1R-SKBR3 cells (Figure 5A, B). Our results also showed that LX-2 cells secrete KPs, and interestingly, this occurred to a greater extent than MDA-MB-231 or KISS1R-SKBR3 cells (Figure 5C).

It was reported that in response to potent profibrogenic factors such as TGFβ activated hepatic stellate cells in the injured liver promote fibrosis by upregulating extracellular proteins such as collagen, smooth muscle actin and fibronectin and tissue inhibitors of metalloproteinases 1 (TIMP-1)[30]. We therefore used this cell model to study the effect of KPA on fibrogenesis. Serum-starved LX-2 cells treated with TGFβ (5 ng/ml) for 48 h upregulated both the mRNA (*COL1A1, FN, ACTA2 and TIMP1*), and protein (collagen and fibronectin) levels of fibrogenic markers, and this upregulation was significantly blocked in the presence of KPA (3 nM) (Figure 5D-J). Furthermore, in primary mouse hepatic stellate cells KPA (3 nM) treatment for 48 h significantly reduced the mRNA expression of profibrogenic markers, *Col1a1,* and *Acta2*, and lowered the expression of *Timp1* (Figure 6).

 doi:10.20944/preprints202409.1111.v1

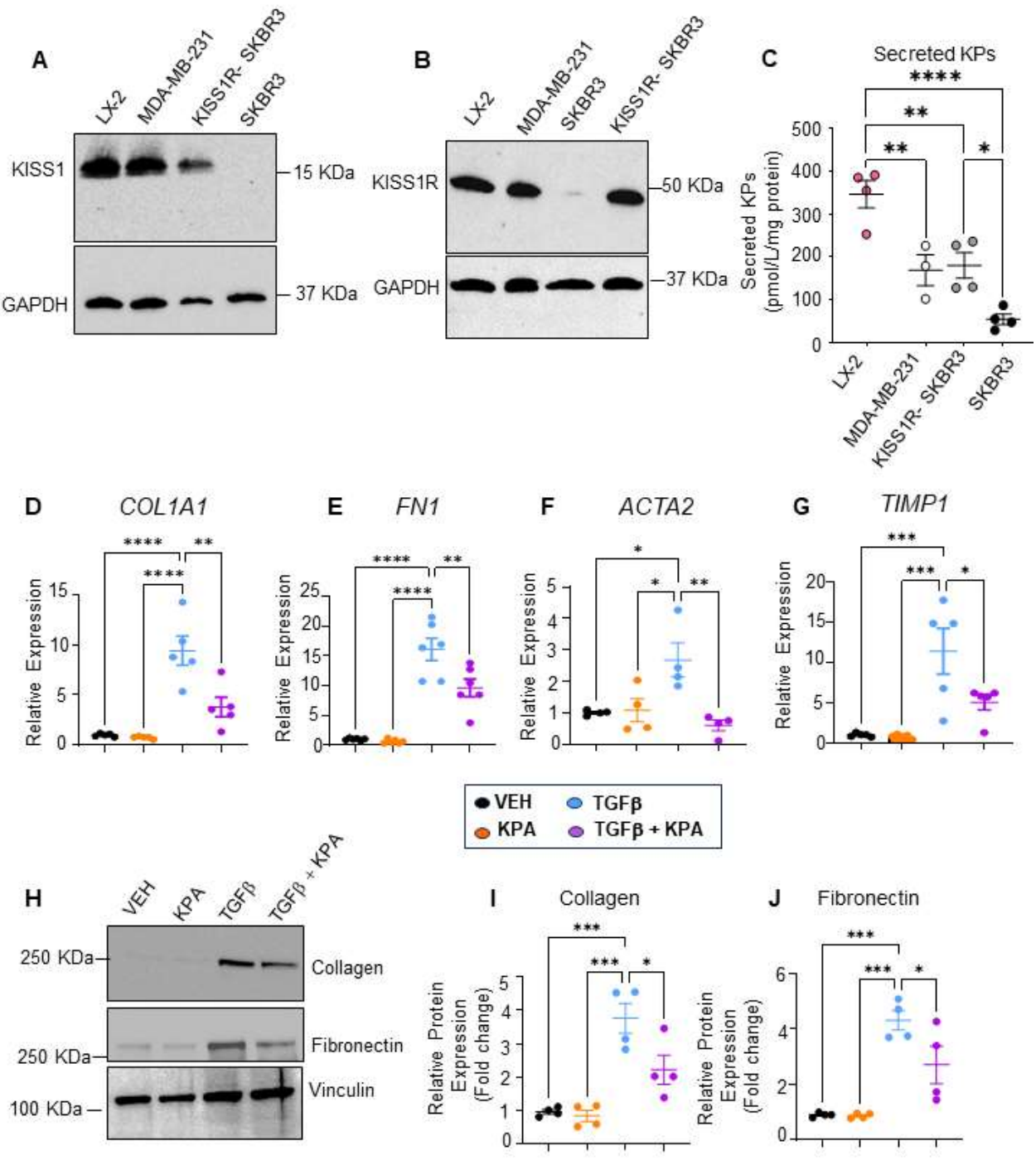

Figure 5. KPA treatment decreases activation of human hepatic stellate LX-2 cells. Western blot analysis of endogenous **(A)** KISS1 protein and **(B)** KISS1R protein expression. MDA-MB-231, SKBR3 and KISS1R-SKBR3 were used as a reference for expression. **(C)** Secreted kisspeptin protein in culture media measured by ELSIA. **(D-G**) Changes in fibrogenic gene expression in response to KPA (3 nM, 48h) +/- TGFβ (5 ng/ml, 48h). **(H)** Western blot analysis and **(I, J)** densitometric analyses of blots, showing changes in fibrogenic protein in response to KPA (3nM, 72h) +/- TGFβ (5 ng/ml, 72h). Results expressed as mean +/- S.E.M. *p < 0.05 vs control. **p < 0.01 vs control. ***p < 0.001 vs control. ****p < 0.0001 vs control. One-way ANOVA followed by multiple comparison test.

Preprints.org (www.preprints.org) | NOT PEER-REVIEWED | Posted: 14 September 2024 doi:10.20944/preprints202409.1111.v1

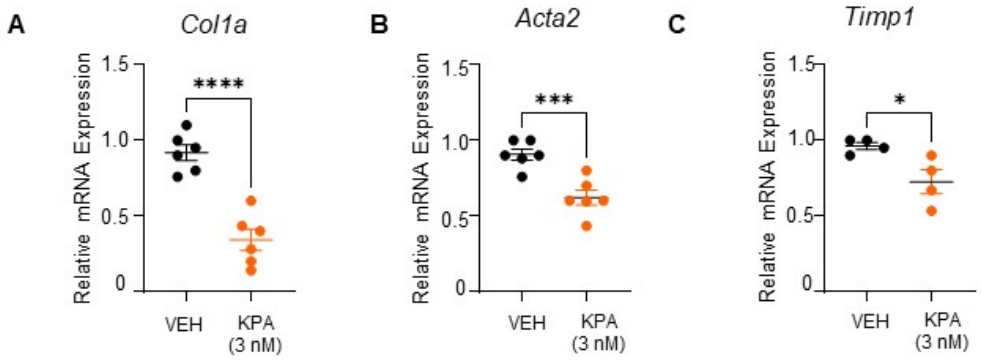

Figure 6. KPA reduces fibrogenic markers in primary mouse HSCs. Gene expression by qPCR analysis showing the effect of KPA (3 nM, 48h) treatment on **(A)** *Col1a*, **(B)** *Acta2* and **(C)** *Timp1.* Results expressed as mean +/- S.E.M. Student's unpaired t test. *p < 0.05 vs control. **p < 0.01 vs control. ***p < 0.001 vs control. ****p < 0.0001 vs control.

Changes in profibrogenic markers in LX-2 cells were confirmed in the RNA-seq datasets at 48 h of treatment with KPA (3 nM) in combination with TGFβ (5 ng/ml), in contrast to cells treated with TGFβ (5 ng/ml) alone (Figure 7A-F). Gene enrichment analysis revealed that pathways regulating the extracellular matrix were downregulated in KPA treated groups in the presence of TGFβ, in contrast to TGFβ alone (Figure 8). KPA treatment also significantly decreased TGFβ-induced increase in leukemia inhibitory factor (*LIF*), and interleukin 11 (*IL11*), two members of IL6 family of cytokines (Figure 7G, H). Co-treatment with KPA also decreased the expression of genes (Figure 7I, J) regulating the progression of fibrosis (e.g *COL6A3, AEBP1, SPARC, TNC, LAMB1, BGN)* and hepatocellular carcinoma (e.g. *COL4A1, COL4A2, TUFT1, VCAN, NID1*).

 doi:10.20944/preprints202409.1111.v1

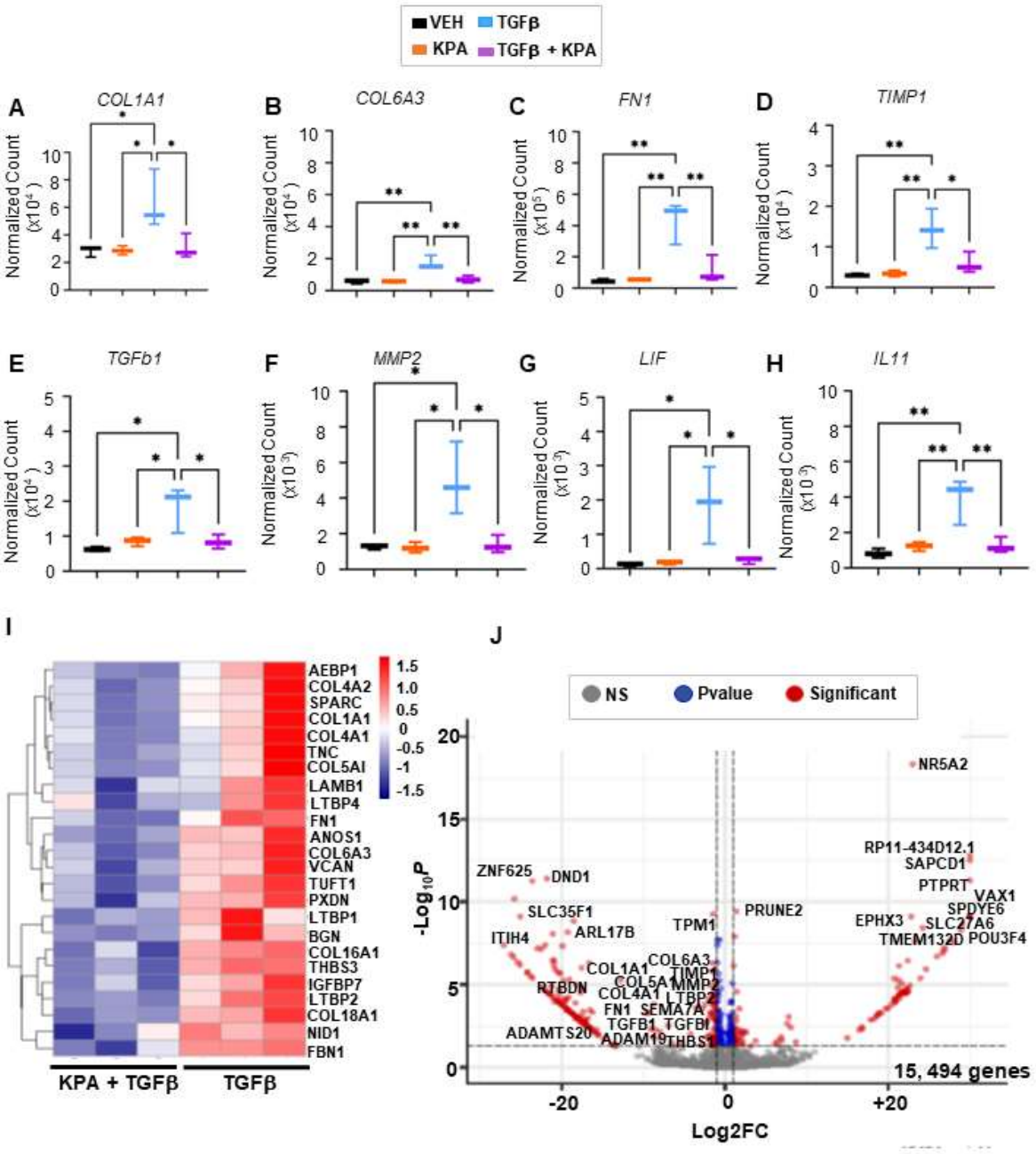

Figure 7. Effect of KPA treatment on gene expression in human hepatic stellate cells by RNA-seq. RNA was extracted from LX-2 cells treated PBS (vehicle), KPA (3 nM, 48h) +/- TGFβ (5 ng/ml, 48h). Changes in fibrogenic (A-F) and inflammatory (G, H) genes by transcriptomic analysis. Data presented as (I) heatmap and (J) volcano plot of differentially expressed genes (padj <0.1) in LX-2 cells treated with KPA (3 nM, 48h) + TGFβ (5 ng/ml, 48h). compared to TGFβ alone. Results expressed as mean +/- S.E.M. *p < 0.05 vs control. **p < 0.01 vs control. One-way ANOVA followed by multiple comparison test.

 doi:10.20944/preprints202409.1111.v1

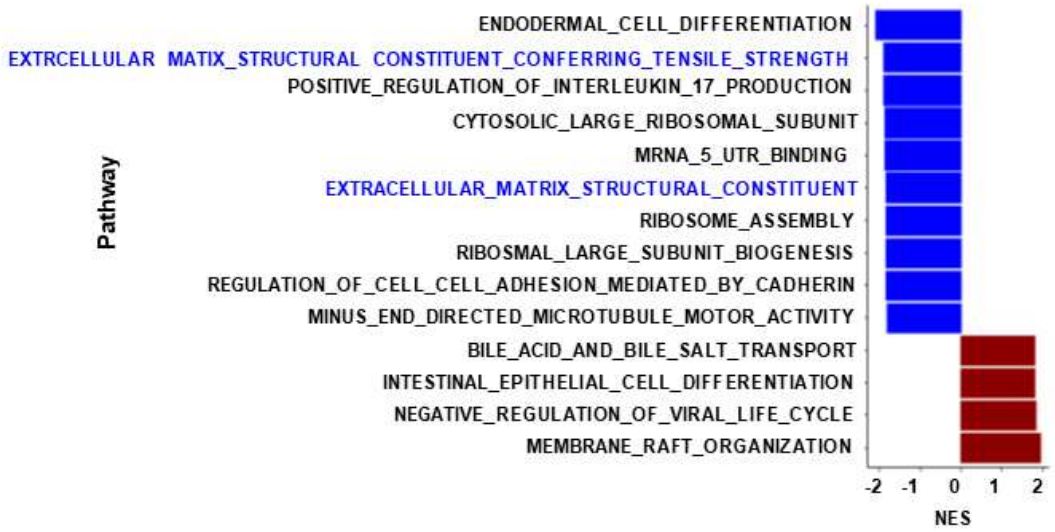

Figure 8. KPA downregulates molecular pathways related to extracellular matrix production in HSCs. Gene set enrichment analysis of LX-2 cells after 48 h of treatment with KPA (3 nM) with TGFβ (5 ng/ml) or TGFβ alone is shown. The x-axis represents normalized enrichment scores of gene sets (blue: downregulated pathways; red: upregulated pathways).

Activated HSCs secrete collagen, which upon deposition leads to fibrosis. We therefore, examined the effect of KPA on TGFβ–induced collagen secretion and found that it was diminished by KPA treatment (3 nM) (Figure 9A). To further understand the cellular action of KPA on LX-2 cells, we conducted cell migration, proliferation and colony formation assays. We found that KPA reduced LX-2 cell migration, as assessed using scratch/wound healing assay (Figure 9B) and decreased cell proliferation as examined by BrdU assay (Figure 9C). It was also observed that KPA (3 nM, 100 nM) decreased LX-2 colony formation on soft agar (Figure 9D) suggesting that KPA inhibits cell transformation. The effect of KPA on the expression of inflammatory markers was also assessed. KPA treatment reduced TGFβ-induced *IL6* expression (Figure 9E) but did not significantly change TGFβ-induced *TNFA* mRNA levels (Figure 9F). Similar to the observations with hPCLS, KPA (100 nM) significantly upregulated *KISS1* and *KISS1R* mRNA levels (Figure 9G, H). Taken together, these findings suggest that KPA directly attenuates hepatic fibrogenesis by decreasing stellate cell activation.

Preprints.org (www.preprints.org) | NOT PEER-REVIEWED | Posted: 14 September 2024 doi:10.20944/preprints202409.1111.v1

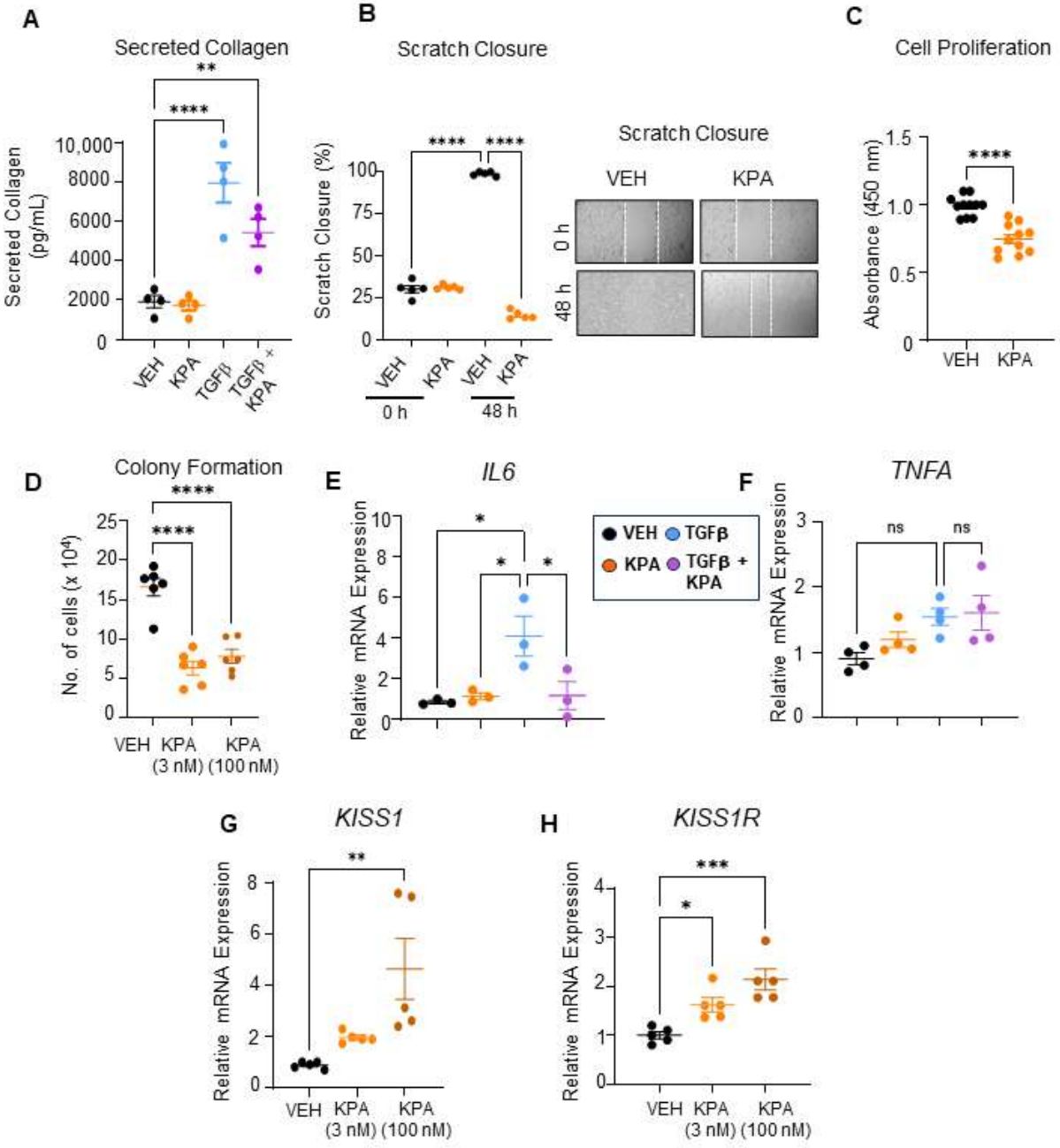

Figure 9. KPA treatment decreases collagen secretion, cell migration and proliferation of LX-2 cells. Quantification of **(A)** TGFβ-induced collagen secretion following VEH, KPA (3 nM), TGFβ (5 ng/ml), KPA+TGFβ treatment, **(B)** cell migration following VEH and KPA (3 nM) treatment. KPA treatment decreases **(C)** LX-2 cell proliferation following VEH and KPA (3 nM) treatment, as assessed using BrdU and **(D)** soft agar colony formation following VEH, KPA (3 nM, 100nM) treatment. Gene expression by qPCR analysis showing the effect of KPA (3 nM, 48h) treatment on inflammatory markers **(E, F)** *IL6* and *TNFA*, and **(G, H)** KISS*1* and *KISS1R*. Results expressed as mean +/- S.E.M. Student's unpaired t-test or one-way ANOVA followed by multiple comparison test. *p < 0.05 vs control. **p < 0.01 vs control. ***p < 0.001 vs control. ****p < 0.0001 vs control.

3.4. KPA Inhibits TGFβ Signaling in Hepatic Stellate Cells via Activation of Protein Phosphatase PP2A

TGFβ is a major profibrogenic cytokine that plays a significant role in hepatic fibrogenesis since it potently induces hepatic stellate cell activation[18; 31]. In canonical TGFβ signaling, TGFβ binding

 doi:10.20944/preprints202409.1111.v1

to the TGFβ type II receptor (TGFβRII) stimulates the recruitment of the TGFβ type I receptor (TGFβRI). TGFβRI then binds and phosphorylates its substrates, receptor-activated SMADs, specifically SMAD2 and SMAD3. These phosphorylated SMADs then forms a heterocomplex with the shared partner, SMAD4. This complex translocates to the nucleus to activate the transcription of multiple target profibrogenic genes such as *COL1A1, ACTA2, FN, TIMP-1, and SNAI1*[18; 32; 33].

To investigate the potential mechanism by which KISS1R signaling improves hepatic fibrogenesis, the effect of KPA on TGFβ1/SMAD signaling was examined in LX-2 cells. Treatment with TGBβ induced the phosphorylation of p-SMAD2/3, which was significantly reduced in the presence of KPA (Figure 10A). TGBβ treatment also resulted in robust expression of its downstream target, SNAIL, a mesenchymal marker that is a critical regulator of hepatic stellate cell activation[33]. KPA treatment attenuated TGBβ induced expression of SNAIL mRNA and protein (Figure 10B, C). KISS1R C-terminal directly binds serine/threonine protein phosphatase type 2A (PP2A)[34]. Activation of PP2A promotes dephosphorylation of SMAD 2/3[35]. We therefore investigated whether pharmacological inhibition of PP2A using okadaic acid (OA) in the presence of kisspeptin interfered with TGBβ-SMAD signaling. Cells were pretreated with OA (5 nM) for 3 h, before introducing TGFβ1 (5 ng) and KPA (3nM) to study SMAD2/3 phosphorylation after 48 hours; OA treatment did not impact cell viability (Figure S5). Western blot analysis revealed that treatment with protein phosphatase inhibitor abolished the effects of KPA on the dephosphorylation of SMAD2/3 (Figure 10D).

Overall, the present data indicate KPA/KISS1R signaling directly suppresses hepatic fibrogenesis by inhibiting TGBβ signaling, through regulating PP2A phosphatases (Figure 10E), thus identifying it as a new therapeutic target to potentially treat fibrosis.

 doi:10.20944/preprints202409.1111.v1

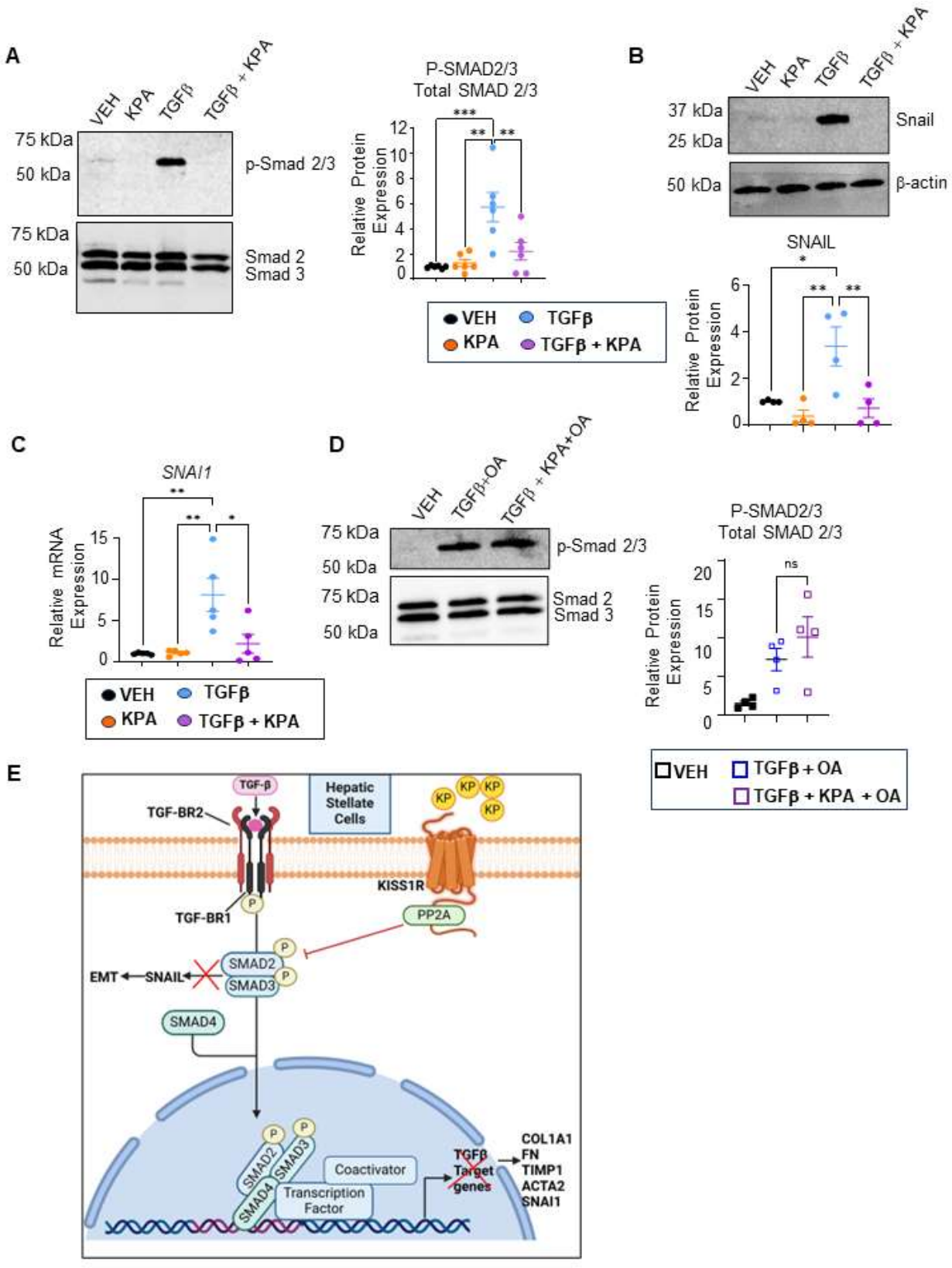

Figure 10. KPA treatment decreases TGFβ signaling in human HSc. **(A)** TGFβ-induced SMAD phosphorylation and **(B)** SNAIL expression, following KPA (3 nM, 72 h) treatment, as determined by Western blot analysis; densitometric analysis of blots are shown below. **(C)** TGFβ-induced *SNAI1* mRNA expression following KPA (3 nM, 48 h) determined by qPCR. **(D)** TGFβ-induced SMAD 2/3 phosphorylation cells were pretreated with OA (5 nM) for 3 h, following TGFβ1 (5 ng/ml) and/or KPA (3 nM) for 48 as determined by Western blot analysis. OA treatment did not impact cell viability (see

 doi:10.20944/preprints202409.1111.v1

Figure S5). **(E)** Schematic showing proposed signaling pathways by which KISS1R activation by kisspeptin (KP) suppresses hepatic fibrosis in hepatic stellate cells. Results expressed as mean +/- S.E.M. *p < 0.05 vs control. **p < 0.01 vs control. ***p < 0.001 vs control. One-way ANOVA followed by multiple comparison test.

4. Discussion

Kisspeptin is well studied as a neuropeptide that critically regulates pubertal and reproductive development by acting on the hypothalamus to stimulate gonadotropin-releasing hormone secretion, and the release of gonadotropins (follicle stimulating and luteinizing hormone) from the pituitary. Hypothalamic KISS1 and KISS1R expression is decreased in many pathological conditions, resulting in the delay or absence of puberty in children, hypogonadotrophic hypogonadism and reproductive disorders[6; 36]. Chronic administration of kisspeptin is safe and can restore normal pubertal development in children with delayed puberty[18] in addition to treating hypothalamic amenorrhea in women, and hyposexual drive disorder in otherwise healthy males[37].

Outside the brain, kisspeptin and its receptor are expressed in tissues such as liver, gonads, uterus, placenta, small intestine and adrenal glands[6; 38]. KISS1 and KISS1R are also expressed in pancreatic islets a and b cells[39; 40]. Administration of kisspeptin to human, mouse, rat and pig isolated pancreatic b cells directly increased glucose stimulated insulin secretion (GSIS)[40]. Acute peripheral administration of kisspeptin in humans, mice, rats and monkeys *in vivo* also resulted in increased GSIS[23; 37]. These studies demonstrate an important role for kisspeptin signaling in regulating glucose homeostasis. Hepatocytes express kisspeptin and KISS1R [11]. In the liver, deletion of *Kiss1r* in hepatocytes augmented glucose intolerance and insulin resistance in a HFD-fed mouse model of MASLD[11], in addition to increasing hepatic steatosis and its progression to MASH [11]. In contrast, treatment of HFD-fed male C57BL6/J mice with KPA for 6 weeks improved insulin sensitivity and glucose tolerance and ameliorated steatosis. To evaluate the impact of KPA administration on advanced MASH and fibrosis, male DIAMOND mice were utilized[11]. These mice when maintained on HFD and sugar water diet recapitulate human MASLD by developing obesity, insulin resistance, fatty liver, steatohepatitis, fibrosis and HCC[16]. It was observed that 6 weeks of KPA administration to these DIAMOND mice improved advanced fibrosis, without a significant change in body weight. Thus, the effect of KPA administration was not due to changes in body weight[11]. Mechanistically, it was observed that hepatic KISS1R signaling decreases hepatic lipogenesis and MASH progression, by activating the master energy sensor, AMP-activated protein kinase (AMPK) and increasing mitochondrial fatty acid oxidation. It was also observed that KPA treated DIAMOND mice livers displayed lower mRNA and protein levels of fibrogenic markers (e.g. TGFβ, SMA, collagen, matrix metalloproteinases (MMP) such as MMP-2, MMP-9 and MMP-13, and decreased levels of inflammatory markers (e.g interleukin 1β), and diminished NFκ-b signaling[11]. However, whether kisspeptin had any impact on regulating human hepatic fibrosis was unknown.

In this study, we provide strong evidence that KPA exhibits an antifibrotic activity, using human precision cut ultrathin liver slices, a relevant *ex vivo* human model of fibrotic liver. HPCLs are a powerful three-dimensional model that maintains the complex organization, cellular heterogeneity, and micro-environment of the liver as well as the pathological characteristics of the human disease[41]. Only fibrotic liver sections obtained from patients with HCC were utilized for this study, as verified by a pathologist (tumors sections were excluded). Male patients were included in this initial study, as MASLD is more prevalent in males than in females[42]. We demonstrate for the first time that KISS1R is strongly expressed in human hepatic stellate cells in fibrotic MASH patient liver biopsies. KISS1 and KISS1R are also expressed in hepatocytes and the liver produces kisspeptin[11; 12]. Thus, attenuating signals from KISS1R expressed in other cell types such as hepatocytes may contribute to the anti-fibrogenic effects of kisspeptin signaling.

KPA, created by modification of kisspeptin-10 (a naturally occurring kisspeptin peptide), exhibits increased stability and potency[43]. As reported here, KPA lowered the expression of fibrogenic markers (*COL1A, FN1, ACTA2*) in hPLCS, decreased collagen secretion and reduced the expression of inflammatory markers (*IL-6, TNFA*). This effect was similar to the TGFβ receptor 1

 doi:10.20944/preprints202409.1111.v1

kinase inhibitor II (Alk5i), which has been shown to have a beneficial effect on MASLD[19; 44]. These results are consistent with our observations made in the DIAMOND mouse model[11], suggesting the antifibrogenic potential of KPA in humans with fibrotic liver disease.

Another major finding from this study was made using human HSCs and primary mouse HSCs where we show for the first time that KPA decreased fibrogenesis through the downregulation of the canonical TGFβ signaling pathway. This led to the decreased expression of TGFβ-target genes *(COL1A, FN-1, TIMP-1, SNAI1)* that are implicated in fibrosis. TGFβ plays a key role in the progression of liver fibrosis, and drugs that inhibit TGFβ have anti-fibrotic effects[18]. We showed that in stellate cells, KPA specifically decreased TGFβ-induced p-SMAD2/3 levels. SMAD2/3 has been shown to mediate extracellular matrix accumulation and fibrosis in the liver[31; 45] and to regulate epithelial-mesenchymal transition (EMT) and metastasis, in response to TGFβ in HCC[46]. We also show that in HSCs, KPA treatment reduced the expression of the profibrogenic, EMT-related transcription factor, SNAIL, which is a TGFβ-target gene[47; 48]. Our data suggest that KPA's effect on promoting dephosphorylation of phospho-SMAD2/3 in the presence of TGFβ1 is mediated at least in part, by increasing the activity of protein phosphatase PP2A, a direct binding partner of KISS1R. Together, these data provide evidence for the involvement of the TGFβ1/SMAD2/3 pathway in the kisspeptin-mediated inactivation of HSC.

Another interesting finding resulting from this study was the observation that KPA upregulates KISS1/KISS1R expression in hPCLS and LX-2, suggesting another mechanism of action by which KPA is mediating its protective effect. This observation is also supported by our current and previous findings that overexpression of KISS1R in SKBR3 cells resulted not only in the increased levels of KISS1R, but also that of KISS1[26]; this has also been reported to occur in human endometrial cells upon exogenous expression of KISS1R[49]. These findings suggest that there is a positive feedback loop between KISS1 and KISS1R. The expression of KISS1 and KISS1R mRNA and protein is low in healthy human liver but increases in liver biopsies from MASH patients compared with those of healthy subjects[11]. Plasma kisspeptin levels are also increased in patients with steatosis and MASH, compared to healthy subjects, suggesting that the upregulation of KISS1R signaling pathway is a compensatory and protective response aiming to resolve MASLD[11]. In further support of this idea, studies in mice showed that liver *Kiss1* expression is increased in genetic models of obesity and type 2 diabetes (db/db and ob/ob mice)[12]. We and others have also observed increased expression of *Kiss1* and *Kiss1r* in a high-fat diet fed mouse model of MASLD[11; 12; 50]. Thus, the upregulation of hepatic KISS1/KISS1R by KPA may serve to slow down or reverse disease progression. Our future studies will investigate the mechanism(s) by which KPA treatment leads to an upregulation of KISS1/KISS1R.

Earlier this year, the thyroid hormone receptor β agonist, Resmetirom was the first drug approved by the FDA to treat MASH, having improved key readouts of liver pathology in 25–30% of patients in phase III clinical trial[51]. This highlights the continuous need for new therapeutics. Our translational observations provide for the first-time evidence for the therapeutic potential of KP peptides in a human setting of MASLD and support the use of KISS1R activating strategies in clinical trials.

Supplementary Material: The following supporting information can be downloaded at the website of this paper posted on Preprints.org.

CRediT Authorship Contribution Statement: Investigation: D.B, K.P, S.S, K.I, T.H, B.M, M.B.B conducted the experiments, evaluated the data, and preparation of the manuscript. Formal analysis: D.B, K.P, S.S, T.H, K.I, M.B.B, Z.Z. Funding acquisition: U.B.P. S.L.F, M.B. Project administration: M.B. Resources: U.B.P. S.L.F, M.B. Supervision: U.B.P. S.L.F, M.B. Writing – review & editing: D.B, K.P, S.S, T.H, B.M, K.I., M.B.B, Z.Z. M.B, U.B.P. S.L.F. M.B. designed the study, revised and analyzed the data, and wrote the manuscript.

Funding: This work was funded by grants to MB: NIH grants 7R01DK129870-03, New Jersey Health Foundation - PC-151-23 and seed grant from the Rutgers NJ Institute for Food Nutrition and Health S.D.G; NIH grants 5R01DK128289-03 (awarded to S.L.F) and DK119767 (awarded to U.B.P).

Institutional Review Board Statement. The hPCLS study was conducted in accordance with the Declaration of Helsinki and approved by Institutional Review Board (IRB) as an exempted study at Icahn School of Medicine

 doi:10.20944/preprints202409.1111.v1

at Mount Sinai, New York City, N.Y. IRB approved by Icahn School of Medicine at Mount Sinai. The animal study protocol was approved by Institutional Animal Care and Use Committee (IACUC) of Rutgers University (protocol PROTO201702536, 7/19/2024) for studies involving animals.

Data Availability Statement: RNA-seq dataset has been deposited to GEO (Gene Expression Omnibus). It will be publicly available once this manuscript is published.

Acknowledgments: Graphics were created using Biorender software. We thank Ms. Yuliya Hapiak for her technical help with the manuscript.

Conflicts of Interest: The funders had no role in the design of the study; in the collection, analyses, or interpretation of data; in the writing of the manuscript; or in the decision to publish the results. MB is a coinventor on a patent application US20230256051A1 filed by Rutgers University. S.L.F has relationships with the companies listed below, however these activities are unrelated to the content of this article: Consulting: 89 Bio, Boehringer Ingelheim, Boston Pharmaceuticals, Bristol Myers Squibb, ChemomAb, Foresite Laboratories, Gordian Biotechnology, Glycotest, Glympse Bio, Hepgene, In sitro, Junevity, Korro Bio, Kriya, Laekna, Lerna Therapeutics, Macomics, Mediar, Merck, Morphic Therapeutics, North Sea Therapeutics, Ochre Bio, Overtone Therapeutics, Pfizer Pharmaceuticals, Pliant, Prosciento, RAPT, Sagimet, Satellite Bio, Seal Rock, Scholar Rock, Sunbird Bio, Surrozen, Takeda, Variant Bio. Stock options: Escient, Galectin, Galmed, Genfit, Gordian Biotechnology, Hepgene, Junevity, Lifemax, Metacrine, Morphic Therapeutics, Nimbus, North Sea, Ochre Bio, Therapeutics, Scholar Rock, Sunbird Bio. Research Activities with Commercial Entities: Abalone Bio (SBIR Grant); Novo Nordisk. The other authors declare no conflicts of interest that pertain to this work.

References

1. Younossi, Z.M., Golabi, P., Paik, J.M., Henry, A., Van Dongen, C., Henry, L., 2023. The global epidemiology of nonalcoholic fatty liver disease (NAFLD) and nonalcoholic steatohepatitis (NASH): a systematic review. Hepatology 77(4):1335-1347.
2. Hagstrom, H., Nasr, P., Ekstedt, M., Hammar, U., Stal, P., Hultcrantz, R., et al., 2017. Fibrosis stage but not NASH predicts mortality and time to development of severe liver disease in biopsy-proven NAFLD. J Hepatol 67(6):1265-1273.
3. Llovet, J.M., Willoughby, C.E., Singal, A.G., Greten, T.F., Heikenwalder, M., El-Serag, H.B., et al., 2023. Nonalcoholic steatohepatitis-related hepatocellular carcinoma: pathogenesis and treatment. Nat Rev Gastroenterol Hepatol 20(8):487-503.
4. Tapper, E.B., Parikh, N.D., 2023. Diagnosis and Management of Cirrhosis and Its Complications: A Review. JAMA 329(18):1589-1602.
5. Noureddin, M., Vipani, A., Bresee, C., Todo, T., Kim, I.K., Alkhouri, N., et al., 2018. NASH Leading Cause of Liver Transplant in Women: Updated Analysis of Indications For Liver Transplant and Ethnic and Gender Variances. Am J Gastroenterol 113(11):1649-1659.
6. Bhattacharya, M., Babwah, A.V., 2015. Kisspeptin: beyond the brain. Endocrinology 156(4):1218-1227.
7. Kirby, H.R., Maguire, J.J., Colledge, W.H., Davenport, A.P., 2010. International Union of Basic and Clinical Pharmacology. LXXVII. Kisspeptin receptor nomenclature, distribution, and function. Pharmacol Rev 62(4):565-578.
8. Li, X., Liang, C., Yan, Y., 2022. Novel Insight into the Role of the Kiss1/GPR54 System in Energy Metabolism in Major Metabolic Organs. Cells 11(19).
9. Wolfe, A., Hussain, M.A., 2018. The Emerging Role(s) for Kisspeptin in Metabolism in Mammals. Front Endocrinol (Lausanne) 9:184.
10. Shoji, I., Hirose, T., Mori, N., Hiraishi, K., Kato, I., Shibasaki, A., et al., 2010. Expression of kisspeptins and kisspeptin receptor in the kidney of chronic renal failure rats. Peptides 31(10):1920-1925.
11. Guzman, S., Dragan, M., Kwon, H., de Oliveira, V., Rao, S., Bhatt, V., et al., 2022. Targeting hepatic kisspeptin receptor ameliorates nonalcoholic fatty liver disease in a mouse model. J Clin Invest 132(10).
12. Song, W.J., Mondal, P., Wolfe, A., Alonso, L.C., Stamateris, R., Ong, B.W., et al., 2014. Glucagon regulates hepatic kisspeptin to impair insulin secretion. Cell Metab 19(4):667-681.
13. Fang, P., She, Y., Zhao, J., Yan, J., Yu, X., Jin, Y., et al., 2021. Emerging roles of kisspeptin/galanin in age-related metabolic disease. Mech Ageing Dev 199:111571.
14. Izzi-Engbeaya, C., Dhillo, W.S., 2022. Emerging roles for kisspeptin in metabolism. J Physiol 600(5):1079-1088.
15. Musa, E., Matjila, M., Levitt, N.S., 2022. Kisspeptins and Glucose Homeostasis in Pregnancy: Implications for Gestational Diabetes Mellitus-a Review Article. Reprod Sci 29(2):321-327.
16. Asgharpour, A., Cazanave, S.C., Pacana, T., Seneshaw, M., Vincent, R., Banini, B.A., et al., 2016. A diet-induced animal model of non-alcoholic fatty liver disease and hepatocellular cancer. J Hepatol 65(3):579-588.

 doi:10.20944/preprints202409.1111.v1

17. Loomba, R., Friedman, S.L., Shulman, G.I., 2021. Mechanisms and disease consequences of nonalcoholic fatty liver disease. Cell 184(10):2537-2564.
18. Dewidar, B., Meyer, C., Dooley, S., Meindl-Beinker, A.N., 2019. TGF-beta in Hepatic Stellate Cell Activation and Liver Fibrogenesis-Updated 2019. Cells 8(11).
19. Paish, H.L., Reed, L.H., Brown, H., Bryan, M.C., Govaere, O., Leslie, J., et al., 2019. A Bioreactor Technology for Modeling Fibrosis in Human and Rodent Precision-Cut Liver Slices. Hepatology 70(4):1377-1391.
20. Palma, E., Doornebal, E.J., Chokshi, S., 2019. Precision-cut liver slices: a versatile tool to advance liver research. Hepatol Int 13(1):51-57.
21. Bhattacharya, D., Becker, C., Readhead, B., Goossens, N., Novik, J., Fiel, M.I., et al., 2021. Repositioning of a novel GABA-B receptor agonist, AZD3355 (Lesogaberan), for the treatment of non-alcoholic steatohepatitis. Sci Rep 11(1):20827.
22. Xu, L., Hui, A.Y., Albanis, E., Arthur, M.J., O'Byrne, S.M., Blaner, W.S., et al., 2005. Human hepatic stellate cell lines, LX-1 and LX-2: new tools for analysis of hepatic fibrosis. Gut 54(1):142-151.
23. Izzi-Engbeaya, C., Comninos, A.N., Clarke, S.A., Jomard, A., Yang, L., Jones, S., et al., 2018. The effects of kisspeptin on beta-cell function, serum metabolites and appetite in humans. Diabetes Obes Metab 20(12):2800-2810.
24. Zhu, C., Kim, K., Wang, X., Bartolome, A., Salomao, M., Dongiovanni, P., et al., 2018. Hepatocyte Notch activation induces liver fibrosis in nonalcoholic steatohepatitis. Sci Transl Med 10(468).
25. Mederacke, I., Dapito, D.H., Affo, S., Uchinami, H., Schwabe, R.F., 2015. High-yield and high-purity isolation of hepatic stellate cells from normal and fibrotic mouse livers. Nat Protoc 10(2):305-315.
26. Blake, A., Dragan, M., Tirona, R.G., Hardy, D.B., Brackstone, M., Tuck, A.B., et al., 2017. G protein-coupled KISS1 receptor is overexpressed in triple negative breast cancer and promotes drug resistance. Sci Rep 7:46525.
27. Dragan, M., Nguyen, M.U., Guzman, S., Goertzen, C., Brackstone, M., Dhillo, W.S., et al., 2020. G protein-coupled kisspeptin receptor induces metabolic reprograming and tumorigenesis in estrogen receptor-negative breast cancer. Cell Death Dis 11(2):106.
28. Cvetkovic, D., Dragan, M., Leith, S.J., Mir, Z.M., Leong, H.S., Pampillo, M., et al., 2013. KISS1R induces invasiveness of estrogen receptor-negative human mammary epithelial and breast cancer cells. Endocrinology 154(6):1999-2014.
29. Niki, T., De Bleser, P.J., Xu, G., Van Den Berg, K., Wisse, E., Geerts, A., 1996. Comparison of glial fibrillary acidic protein and desmin staining in normal and CCl4-induced fibrotic rat livers. Hepatology 23(6):1538-1545.
30. Park, S.A., Kim, M.J., Park, S.Y., Kim, J.S., Lim, W., Nam, J.S., et al., 2015. TIMP-1 mediates TGF-beta-dependent crosstalk between hepatic stellate and cancer cells via FAK signaling. Sci Rep 5:16492.
31. Yoshida, K., Matsuzaki, K., Murata, M., Yamaguchi, T., Suwa, K., Okazaki, K., 2018. Clinico-Pathological Importance of TGF-beta/Phospho-Smad Signaling during Human Hepatic Fibrocarcinogenesis. Cancers (Basel) 10(6).
32. Moon, H., Ju, H.L., Chung, S.I., Cho, K.J., Eun, J.W., Nam, S.W., et al., 2017. Transforming Growth Factor-beta Promotes Liver Tumorigenesis in Mice via Up-regulation of Snail. Gastroenterology 153(5):1378-1391 e1376.
33. Scarpa, M., Grillo, A.R., Brun, P., Macchi, V., Stefani, A., Signori, S., et al., 2011. Snail1 transcription factor is a critical mediator of hepatic stellate cell activation following hepatic injury. Am J Physiol Gastrointest Liver Physiol 300(2):G316-326.
34. Evans, B.J., Wang, Z., Mobley, L., Khosravi, D., Fujii, N., Navenot, J.M., et al., 2008. Physical association of GPR54 C-terminal with protein phosphatase 2A. Biochem Biophys Res Commun 377(4):1067-1071.
35. Rizvi, F., Siddiqui, R., DeFranco, A., Homar, P., Emelyanova, L., Holmuhamedov, E., et al., 2018. Simvastatin reduces TGF-beta1-induced SMAD2/3-dependent human ventricular fibroblasts differentiation: Role of protein phosphatase activation. Int J Cardiol 270:228-236.
36. Millar, R.P., Babwah, A.V., 2015. KISS1R: Hallmarks of an Effective Regulator of the Neuroendocrine Axis. Neuroendocrinology 101(3):193-210.
37. Patel, B., Koysombat, K., Mills, E.G., Tsoutsouki, J., Comninos, A.N., Abbara, A., et al., 2024. The Emerging Therapeutic Potential of Kisspeptin and Neurokinin B. Endocr Rev 45(1):30-68.
38. Radovick, S., Babwah, A.V., 2019. Regulation of Pregnancy: Evidence for Major Roles by the Uterine and Placental Kisspeptin/KISS1R Signaling Systems. Semin Reprod Med 37(4):182-190.
39. Hauge-Evans, A.C., Richardson, C.C., Milne, H.M., Christie, M.R., Persaud, S.J., Jones, P.M., 2006. A role for kisspeptin in islet function. Diabetologia 49(9):2131-2135.
40. Bowe, J.E., Foot, V.L., Amiel, S.A., Huang, G.C., Lamb, M.W., Lakey, J., et al., 2012. GPR54 peptide agonists stimulate insulin secretion from murine, porcine and human islets. Islets 4(1):20-23.
41. Dewyse, L., Reynaert, H., van Grunsven, L.A., 2021. Best Practices and Progress in Precision-Cut Liver Slice Cultures. Int J Mol Sci 22(13).

 doi:10.20944/preprints202409.1111.v1

42. Lonardo, A., Nascimbeni, F., Ballestri, S., Fairweather, D., Win, S., Than, T.A., et al., 2019. Sex Differences in Nonalcoholic Fatty Liver Disease: State of the Art and Identification of Research Gaps. Hepatology 70(4):1457-1469.
43. Asami, T., Nishizawa, N., Matsui, H., Nishibori, K., Ishibashi, Y., Horikoshi, Y., et al., 2013. Design, synthesis, and biological evaluation of novel investigational nonapeptide KISS1R agonists with testosterone-suppressive activity. J Med Chem 56(21):8298-8307.
44. Kostadinova, R., Strobel, S., Chen, L., Fiaschetti-Egli, K., Gadient, J., Pawlowska, A., et al., 2024. Digital pathology with artificial intelligence analysis provides insight to the efficacy of anti-fibrotic compounds in human 3D MASH model. Sci Rep 14(1):5885.
45. Koo, J.H., Lee, H.J., Kim, W., Kim, S.G., 2016. Endoplasmic Reticulum Stress in Hepatic Stellate Cells Promotes Liver Fibrosis via PERK-Mediated Degradation of HNRNPA1 and Up-regulation of SMAD2. Gastroenterology 150(1):181-193 e188.
46. Yang, Y., Liu, Q., Li, Z., Zhang, R., Jia, C., Yang, Z., et al., 2018. GP73 promotes epithelial-mesenchymal transition and invasion partly by activating TGF-beta1/Smad2 signaling in hepatocellular carcinoma. Carcinogenesis 39(7):900-910.
47. Liu, M., Peng, P., Wang, J., Wang, L., Duan, F., Jia, D., et al., 2015. RACK1-mediated translation control promotes liver fibrogenesis. Biochem Biophys Res Commun 463(3):255-261.
48. Song, Y., Kim, S., Heo, J., Shum, D., Lee, S.Y., Lee, M., et al., 2021. Identification of hepatic fibrosis inhibitors through morphometry analysis of a hepatic multicellular spheroids model. Sci Rep 11(1):10931.
49. Schaefer, J., Chadchan, S.B., George, A.F., Roan, N.R., Bhattacharya, M., Kommagani, R., et al., 2022. Human endometrial KISS1R inhibits stromal cell decidualization in a manner associated with a reduction in ESR1 levels. bioRxiv:2022.2011.2020.517219.
50. Dudek, M., Kolodziejski, P.A., Pruszynska-Oszmalek, E., Sassek, M., Ziarniak, K., Nowak, K.W., et al., 2016. Effects of high-fat diet-induced obesity and diabetes on Kiss1 and GPR54 expression in the hypothalamic-pituitary-gonadal (HPG) axis and peripheral organs (fat, pancreas and liver) in male rats. Neuropeptides 56:41-49.
51. Harrison, S.A., Bedossa, P., Guy, C.D., Schattenberg, J.M., Loomba, R., Taub, R., et al., 2024. A Phase 3, Randomized, Controlled Trial of Resmetirom in NASH with Liver Fibrosis. N Engl J Med 390(6):497-509.